Hindawi Publishing Corporation
Mathematical Problems in Engineering
Volume 2014, Article ID 607520, 5 pages
http://dx.doi.org/10.1155/2014/607520

Research Article

Optimization of Tungsten Carbide Opposite Anvils Used in the In Situ High-Pressure Loading Apparatus

Zhang Ying,[1,2] Chen Xiping,[1] Sun Guangai,[1] Lu Yuping,[3] Gong Jian,[1] and He Duanwei[3]

[1] *Key Laboratory for Neutron Physics of Chinese Academy of Engineering Physics, Institute of Nuclear Physics and Chemistry, Mianyang 621900, China*
[2] *School of Nuclear Science and Technology, University of Science and Technology of China, Hefei 230026, China*
[3] *Institute of Atomic and Molecular Physics, Sichuan University, Chengdu 610065, China*

Correspondence should be addressed to Zhang Ying; zhangying_china@163.com

Received 23 March 2014; Revised 26 May 2014; Accepted 16 June 2014; Published 29 June 2014

Academic Editor: Sergio Preidikman

In order to optimize the structure of anvils, finite element method is used to simulate two kinds of structures, one of which has a support ring but the other one does not. According to the simulated results, it is found that the maximum value of pressure appears at the center of culet when the bevelled angle is about 20°. Comparing the results of these two kinds of structures, we find that the efficiency of pressure transformation for the structure without support ring is larger than that for the structure with support ring. Considering the effect of von Mises stress, two kinds of tungsten carbide opposite anvils have been manufactured with bevelled angle of 10°. The experimental results for these two anvils are in good agreement with the simulation.

1. Introduction

By employing neutron diffraction technique with in situ high-pressure loading apparatus, it is accessible to detect on time the phase transition, strength, and texture of materials under extreme high pressure. As a powerful characterization method, this kind of in situ neutron diffraction technique has shed light on microstructure and properties of complex compounds [1–6].

The development of this technique benefited from the progress of opposite high-pressure apparatus. Introduction of diamond anvil cell has revolutionized the study of materials under extreme high pressure [7]. As the crucial part of this apparatus, the structure of anvils affects directly the performance of the device. In the high-pressure experiment, the stress is concentrated on the sample through bevelled diamonds, which is allowed to reach several mega bars [8–11]. However, the diamond anvil can access the high pressure only for small samples, which excludes some special experiments. Multianvil devices that employ tungsten or silicon carbide anvils could accommodate to much larger sample volumes than the diamond anvil cells under high pressure [12]. It was well known that the stress distribution affects the performance of anvils. Unfortunately, the stress distribution on anvils cannot be obtained in the experimental manner. Many studies have been performed on the structure design by using multimaterials for a high-pressure apparatus. However, it is difficult to manufacture the material for anvil. In addition, this type of material is rather expensive. Therefore, to obtain the optimized structure parameters for design, it is worthwhile to investigate carefully the stress distribution with various geometric structures by using finite element stress analysis methods.

Up to now, much attention has been paid to the finite element analysis, for studying the relationship between the structure of anvils and the pressure. The relationship between the stress and strain of diamond anvils has been analysed by the finite element modeling [11], which provides a method to determine the pressure dependence on the yield strength of strong materials used in the gasket. Han et al. have completed the von Mises stress analysis on tungsten carbide anvil used in cubic high-pressure apparatus (CHPA) [13, 14]. Meanwhile, it is found that the double bevelled anvil is more effective than the single one to generate the same sample pressure.

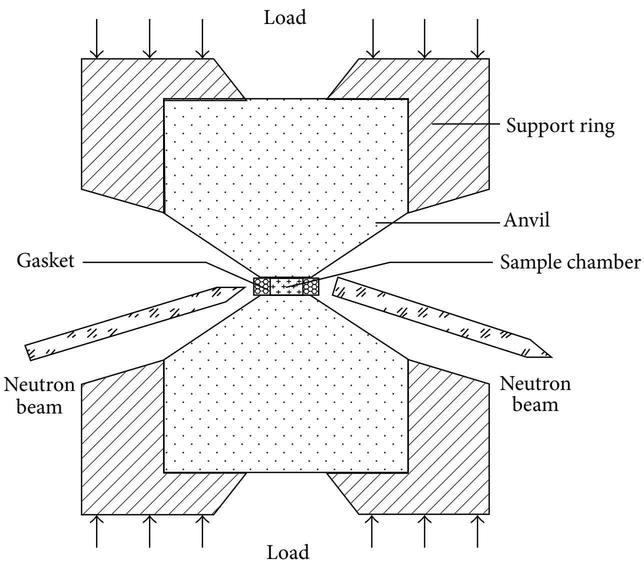

Figure 1: Schematic diagram of in situ high-pressure loading apparatus for neutron scattering experiment.

Bruno and Dunn have attempted to study the optimum configuration of a bevelled single-crystal diamond anvil, finding that the optimum bevelled angle necessary to minimize this stress seems to lie in the neighborhood of 15° [15]. However, the optimum configuration of a bevelled tungsten carbide anvil used in opposite high-pressure apparatus has not been investigated yet.

2. Modeling and Simulation

The high-pressure loading apparatus mentioned in the present paper is designed as the normal MAO-BELL type structure, which is schematically shown in Figure 1. It contains two matched support rings, two opposite anvils, and a gasket between them. In the middle of gasket is a small sample chamber, which is filled with the sample. The pressure is loaded on the bottom of support ring through the press cell. The sample would be in the high-pressure environment based on principle of pressure transmission. Incident neutron beam passes through gasket and is scattered by the sample inside it. The scattered neutron beam reflecting the microstructure information is finally received by detectors of neutron diffraction spectrometer.

The simulation model contains two parts: a bevelled anvil and a pyrophyllite gasket. In particular, two kinds of anvils are made, one of which has the support ring and the other one does not. The material parameters used in the simulation are shown in Table 1. In these cells, the pavilion angle and radius of culet and anvil are constant. So the pavilion height changes along with the bevelled angle. In order to compare the different anvil configurations, the thickness of the gasket is set to be 1 mm, and the applied pressure load along the top of each support ring is uniformly 12 tons. Meanwhile, the shape of support ring is kept in the same dimension. Thus, the optimized parameter for the bevelled angle can be determined under a given loading.

Figure 2(a) shows the novel anvil without additional support ring (anvil combined with support ring), and Figure 2(b) shows the traditional structure anvil with support ring, respectively. The overall dimensions of these two kinds of models are the same. The angle of support ring (α) and pavilion angle (β) are fixed to 15° and 30°, respectively. The range of the bevelled angle (θ) is from 0 to 30°. The radius of culet (r) is 2 mm, and the radius (R) and height (h) of models are 11.5 mm and 5 mm, respectively. The height (n) and radius (m) of traditional anvil are 4 mm and 5.5 mm, respectively.

As mentioned above, two kinds of structures are considered for the finite element models which are, respectively, with and without the support ring. An elastic-plastic analysis is conducted on the anvils. A perfectly cohesive interface is supposed to exist between the anvil and gasket. Solid 95 is chosen as element type; choose target 170 and contact 174 as target surface type and contact surface type in ANSYS software. For the structure with a support ring, a uniform pressure load is applied along the underside of anvil or support ring. The axial cross-section of anvils is circular, and the finite model of 1/2 its semisectional view is shown as in Figure 3. Thanks to the symmetry, stress distribution on the whole anvil is the same as the structure given in Figure 3, which significantly simplifies the computation and the analysis. All nodal points along the center line of the pyrophyllite block are constrained so that only phase displacement along the radial direction is allowed.

3. Results and Discussion

For the case of a uniform pressure over a circular area on a semi-infinite slab [17], there is an intimate relation between the vertical stress σ and the sample pressure P at the center of cullet, which can be expressed as follows: $-P = \sigma$. Therefore, only vertical stress along the axis of the anvil is focused on in the present work. Vertical stress can be obtained by simulation. Then, the changing trend of sample pressure can be found out by the adjusting of structure indirectly.

Figure 4 shows the relationship between vertical stress at the center of culet and bevelled angles under load as 12 ton. It is obvious that the vertical stress varies with the bevelled angle from 0° to 30°. Obviously, the anvils without support ring have larger pressure transmission efficiency than those with the support ring. Anymore, the variation trend with two kinds of anvils is similar. The vertical stress increases gradually with the bevelled angle within the range from 0° to 20°. The maximum value of vertical stress appears at 20°. This observation is consistent with that provided by Bruno and Dunn [15]. However, no more results were supplied by them when the bevelled angle is larger than 20°. Within this range, it is found in the present work that the oscillation of vertical stress appears. In other words, the trend changes irregularly. When the bevelled angle was up to 30°, which is equal to the pavilion angle, the bevelled angle had no signification to decrease shear stress at the corner of anvil.

Table 1: The material parameters used in the simulation [16].

Model	Material	Young's modulus (GPa)	Poisson ratio	Density (kg m^{-3})
Anvil	YG8	600	0.22	1.5 × 104
Support ring	45CrNiMoVA	206	0.30	7.9 × 103
Gasket	Pyrophyllite	5.42	0.12	—

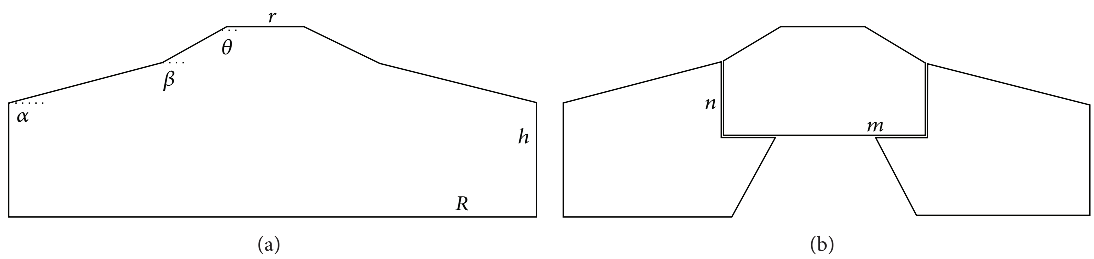

Figure 2: Schematic configuration of tungsten carbide anvils (a) without and (b) with support ring.

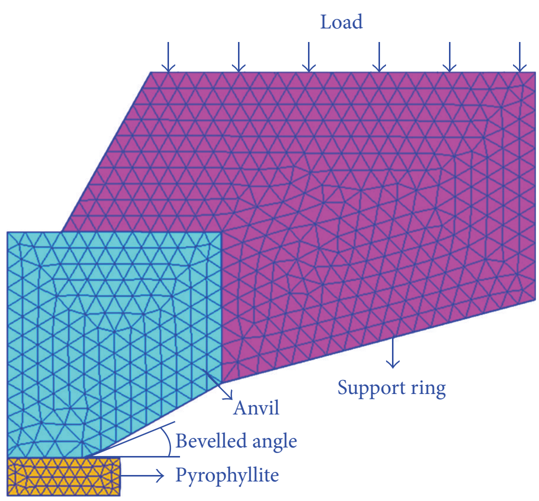

Figure 3: The finite model of its semisectional view.

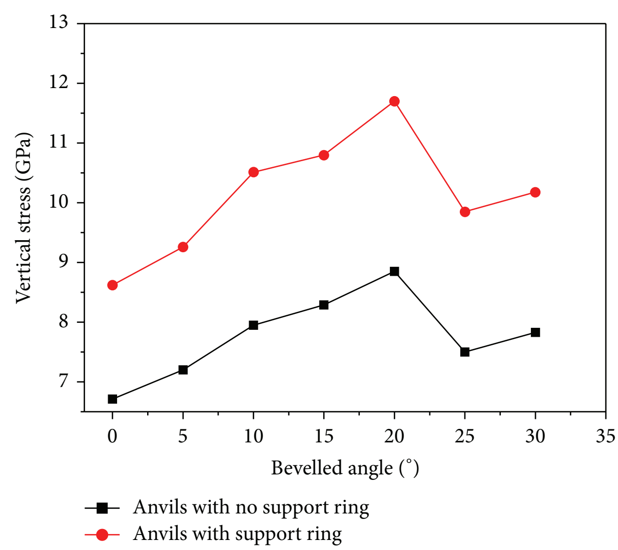

Figure 4: Relationship between the bevelled angles and the vertical stress.

In addition, we observe that stress increases from the center to the edge of culet under high-pressure load. The concentration region of vertical stress isoline is not identical if the bevelled angle changed. Considering the increment range of vertical stress, it is from 20% to 35%. That is similar to the conclusion provided by Forsgren and Drickamer [18].

It has been proved that the shear stress determines the usage life of anvil [14, 19]. If the shear stress is larger than the yield strength, the anvil will be broken [20].

Based on the simulation result, we find that the maximum value of shear stress appears at the edge of anvil face. Its value decreases from the edge to the center. Anymore, we find that the von Mises stress has intimate relations to the vertical stress that has similar changing trend, which has been referred to by Han et al. [14]. When the bevelled angle is about 20°, the von Mises stress reached 14 GPa and 13.1 GPa, respectively.

Considering that the maximum value of von Mises stress increases the risk of causing broken anvils, we set the bevelled angle to 10° and manufacture two kinds of anvils, whose shapes are the same as simulated models mentioned above. Then, we carry out a series of high-pressure experiments using pyrophyllite as the gasket. The normal way to test the high pressure is based on Bridgeman's research that chooses Bi and ZnTe as the materials to identify pressure, because these kinds of materials cause phase transition at special pressure [21].

The information shown in Table 2 expresses different sample chamber pressure corresponding to the extra load with different anvils using ZnTe or Bi. These values such as 5.5 GPa, 9.6 GPa, and 12.6 GPa are three phase transition points of ZnTe. To reach these pressures, extra loads are requested as 7.8 ton, 11.2 ton, and 13.8 ton using model A, respectively. Similarly, the values such as 2.55 GPa, 2.7 GPa, and 7.7 GPa are three phase transition points of Bi. To reach these pressures, extra loads are requested as 5.5 ton, 8.0 ton,

Table 2: The relationship between extra load and sample chamber pressure for models A and B.

ZnTe (phase transition)	Extra load (ton)	Pressure (GPa)	Bi (phase transition)	Extra load (ton)	Pressure (GPa)
I-II	7.8	5.5 (**6.1**)	I-II	5.5	2.55 (**3.05**)
II-III	11.2	9.6 (**10.2**)	II-III	8.0	2.7 (**3.4**)
III-IV	13.8	12.6 (**13.0**)	III-IV	12.0	7.7 (**7.95**)

and 12 ton using model B, respectively. Those values in brackets represent simulation results with the same extra load.

According to the information, we could deduce two conclusions. The first one is that these simulated results are essentially consistent with the experiment data. However, it is obvious that whole simulation results are larger than experiment results. We ascribe this phenomenon to deviations in experiment progress, because we defined that every part in the system was perfectly contacted in simulation model. However, a perfectly cohesive interface is not actual in experiments. It is inevitable to introduce pressure loss. The second one is that model A has larger pressure transmission efficiency than model B. Analyzing the reason that resulted in this phenomenon, we focus on two factors. One is the effect that comes from different hardness of support ring and the other one is the pressure loss at contact surface between anvil and support ring. In order to judge the influence, we design the third anvil C with support ring using WC material and bevelled angle as 10°. A series of simulation experiments under different load were developed. Comparing the chamber pressure in different loading situation, we could find what introduced this effect.

In Figure 5, the curves with labels A, B, and C present relationships between the extra load and the chamber pressure using model A, model B, and the novel model C, respectively. In order to facilitate discussion, we divide four regions in abscissa range. It is obvious that the slopes of three curves in area II are larger than those in area I. We infer that this phenomenon comes from structure preload. In the areas II, III, and IV, three curves show different trends. Curve A approaches to a straight line, but curves B and C do not. In the area III, the growth trend of curves B and C slows down significantly. Considering this phenomenon, we think it comes from pressure loss at contact surface between anvil and support ring. In addition, the overall trend of curve C is higher than curve B. We deduce it to higher hardness of support ring. In other words, it is visible that the impact on the chamber pressure introduced by hardness of support ring is larger than pressure loss at contact surface.

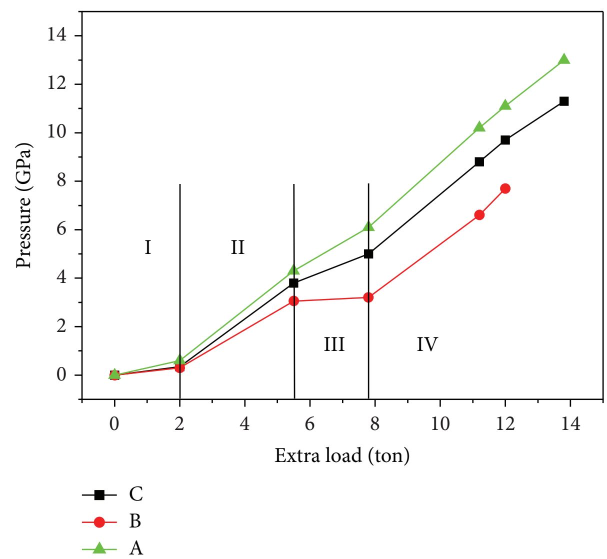

Figure 5: Relationship between the extra load and the chamber pressure using three kinds of anvils.

4. Summary

In this paper, a computational method that simulates stress distribution on tungsten carbide anvils used in opposite high-pressure loading apparatus has been performed. We obtain that the opposite value of vertical stress is equal to the sample pressure at the center of culet. After completing a series of simulations, we deduce that the sample pressure generated by utilizing the structure of anvil with no support ring is higher than the structure of anvil with support ring. Comparing the simulation results and high-pressure experiment results of anvils with bevelled angle as 10°, we find that relationships between them were similar. This conclusion is efficient to provide that this method introduced in this paper is correct. Utilizing this simulated method, people could obtain the optimum structure of anvils used in high-pressure opposite apparatus easily. Based on these novel ways, in situ high-pressure neutron diffraction technology would be much more powerful method to analyse the microstructure and properties of complex compounds.

Conflict of Interests

The authors declare that there is no conflict of interests regarding the publication of this paper.

References

[1] Y. Zhao, J. Zhang, H. Xu et al., "High-pressure neutron diffraction studies at LANSCE," *Applied Physics A*, vol. 99, no. 3, pp. 585–599, 2010.

[2] F. Amita and A. Onodera, "High-pressure cell for neutron scattering under cryogenic temperature and high magnetic field: the Osaka–Kyoto cell," *Review of Scientific Instruments*, vol. 69, article 2738, 1998.

[3] J. Kohlbrecher, A. Bollhalder, R. Vavrin, and G. Meier, "A high pressure cell for small angle neutron scattering up to 500 MPa in combination with light scattering to investigate liquid samples," *Review of Scientific Instruments*, vol. 78, no. 12, Article ID 125101, 2007.

[4] J. Abe, M. Arakawa, T. Hattori et al., "A cubic-anvil high-pressure device for pulsed neutron powder diffraction," *Review of Scientific Instruments*, vol. 81, Article ID 043910, 2010.

[5] L. Y. Tang, L. Lei, L. Jing et al., "Equation of state of tantalum up to 133 GPa," *Chinese Physics Letters*, vol. 27, no. 1, Article ID 016402, 2010.

[6] D. W. Fan, M. Mai-Ning, Y. Jun-Jie et al., "*In Situ* high-pressure synchrotron X-ray diffraction study of clinozoisite," *Chinese Physics Letters*, vol. 28, no. 12, Article ID 126103, 2011.

[7] K. A. Gschneider and Metallurgical Society of AIME, *Metallury at High Pressure and High Temperatures*, p. 10, Gordon and Breach, New York, NY, USA, 1964.

[8] H. Mao and P. Bell, *Year Book*, vol. 76, Carnegie Institute, Washington, DC, USA, 1977.

[9] H. K. Mao and P. M. Bell, "High-pressure physics: sustained static generation of 1.36 to 1.72 megabars," *Science*, vol. 200, no. 4346, pp. 1145–1147, 1978.

[10] P. M. Bell, H. K. Mao, and K. Goettel, "Ultrahigh pressure: beyond 2 megabars and the ruby fluorescence scale," *Science*, vol. 226, no. 4674, pp. 542–544, 1984.

[11] S. Merkel, R. J. Hemley, and H. Mao, "Finite-element modeling of diamond deformation at multimegabar pressures," *Applied Physics Letters*, vol. 74, no. 5, pp. 656–658, 1999.

[12] J. Xu and H.-K. Mao, "Moissanite: a window for high-pressure experiments," *Science*, vol. 290, no. 5492, pp. 783–785, 2000.

[13] Q.-G. Han, Q. Zhang, M.-Z. Li, X.-P. Jia, Y.-F. Li, and H.-A. Ma, "An effective solution for best set of beveling parameters of the cubic high-pressure WC anvil," *Chinese Physics Letters*, vol. 29, no. 11, Article ID 112601, pp. 1–3, 2012.

[14] Q. G. Han, H. Ma, and L. Zhou, "Finite element design of double bevel anvils of large volume cubic high pressure apparatus," *Review of Scientific Instruments*, vol. 78, Article ID 113906, 2007.

[15] M. S. Bruno and K. J. Dunn, "Stress analysis of a beveled diamond anvil," *Review of Scientific Instruments*, vol. 55, no. 6, pp. 940–943, 1984.

[16] Q. G. Han, H. Ma, and R. Li, "Finite element analysis of high-pressure anvils according to the principle of lateral support," *Journal of Applied Physics*, vol. 102, Article ID 084504, 2007.

[17] A. L. Ruoff and H. Luo, "Beam divergence from sharp emitters in a general longitudinal magnetic field," *Journal of Applied Physics*, vol. 70, no. 1, p. 4, 1991.

[18] K. F. Forsgren and H. G. Drickamer, "Design variables for a high pressure cell with supported taper pistons," *Review of Scientific Instruments*, vol. 36, no. 12, pp. 1709–1712, 1965.

[19] J. Xu, H. K. Mao, R. J. Hemley, and E. Hines, "Large volume high-pressure cell with supported moissanite anvils," *Review of Scientific Instruments*, vol. 75, no. 4, Article ID 1034, 2004.

[20] C. Y. Jiang, H. J. Zhang, and Z. Z. Li, *Elasticity Theory and Finite Element Method*, Science, Beijing, China, 2006.

[21] H. K. Wang, D. He, N. Tan et al., "Note: an anvil-preformed gasket system to extend the pressure range for large volume cubic presses," *The Review of Scientific Instruments*, vol. 81, no. 11, Article ID 116102, 2010.